Direct measurement of ^{11}B$(p,\gamma)^{12}$C astrophysical S factors at low energies

J. J. He,[1,2] B. L. Jia,[1,3] S. W. Xu,[1,3,*] S. Z. Chen,[4] S. B. Ma,[1,3] S. Q. Hou,[1] J. Hu,[1,†] L. Y. Zhang,[1,‡] and X. Q. Yu[1]

[1]*Institute of Modern Physics (IMP), Chinese Academy of Sciences, Lanzhou 730000, China*

[2]*Key Laboratory of Optical Astronomy, National Astronomical Observatories, Chinese Academy of Sciences, Beijing 100012, China*

[3]*University of Chinese Academy of Sciences, Beijing 100049, China*

[4]*Institute of Nuclear Energy Safety Technology, Chinese Academy of Sciences, P.O. Box 1135, Hefei 230031, China*

(Received 5 February 2016; revised manuscript received 16 March 2016; published 11 May 2016)

We directly measure the absolute cross section of ^{11}B$(p,\gamma)^{12}$C in the energy region of $E_{\text{c.m.}} = 130$–257 keV by using a thin target for the first time. This work is performed on a 320-kV platform at the Institute of Modern Physics in Lanzhou. The astrophysical S factors of this reaction are obtained for capture to the ground and first excited states of ^{12}C. The properties of the known resonance at ∼150 keV are derived and agree with the previous results. However, in the energy region of 170–240 keV, our S factors are about 15%–50% larger than the adopted values in NACRE II and are also larger than the upper limits of NACRE II by up to ∼20%. This indicates that our new reaction rate is enhanced by about 15%–50% compared to the NACRE II adopted rate in the temperature region 0.32–0.62 GK.

DOI: 10.1103/PhysRevC.93.055804

I. INTRODUCTION

Theoretical models of stellar evolution predict negligible quantities of ^{6}Li, ^{9}Be, and ^{11}B in the hydrogen burning phases of a star's evolution [1]. The primordial big-bang nucleosynthesis (BBN) model might be more generous in its production of these elements [2]. The radiative-capture cross section for proton capture on ^{11}B leading to ^{12}C is small at astrophysically interesting energies because of the large Coulomb barrier. For this reason the proton capture on ^{11}B is often neglected in BBN, and ^{12}C creation is assumed to proceed by neutron capture on ^{11}B followed by subsequent β decay of ^{12}B. In addition, the ^{4}He density produced in the pp chain is high so that the 3α reaction is responsible for generating most of the ^{12}C nuclei in stellar nucleosynthesis. However, proton capture on ^{11}B cannot be entirely neglected in these scenarios. It is thus necessary to measure the ^{11}B$(p,\gamma)^{12}$C reaction cross section (or astrophysical S factor) in the low-energy region of astrophysical interest.

As for the ^{11}B$(p,\gamma)^{12}$C reaction, the properties of a narrow, ∼5-keV-wide, capture resonance at $E_p \approx 163$ keV (i.e., center-of-mass energy $E_{\text{c.m.}} \approx 150$ keV) have been studied in many experiments [3–12], almost all with a thick target because of the low proton energy of this resonance and its narrow width (e.g., see compilation [13]). Although different peak cross sections for this resonance were obtained in different thick-target experiments, i.e., 158 ± 23 μb in Ref. [6], 125 ± 16 or 167 ± 22 μb in Ref. [8], and 139 ± 20 μb in Ref. [12], they are consistent within the uncertainties. Recently, Kelley *et al.* [14] studied this reaction with a polarized proton beam. The cross sections and vector analyzing powers at 90° were determined as a function of the energy for capture to the ground and first excited states of ^{12}C. Their results were used to produce a reliable extrapolation of the astrophysical $S(0)$ factor at zero energy by means of a direct-capture-plus-resonances model calculation. The astrophysical S factor and the thermonuclear reaction rate of the ^{11}B$(p,\gamma)^{12}$C reaction have been compiled in both NACRE I [15] and NACRE II [16]. In this work, we have directly measured the absolute cross section of the ^{11}B$(p,\gamma)^{12}$C reaction in the energy region of $E_{\text{c.m.}} = 130$–257 keV by using a *thin target* for the first time.

II. EXPERIMENT

The experiment was performed at the 320-kV platform [17,18] for multidisciplinary research with highly charged ions at the Institute of Modern Physics (IMP) in Lanzhou. The reaction cross section (or S factor) of the ^{11}B$(p,\gamma)^{12}$C reaction has been measured in the proton energy range of $E_{\text{c.m.}} = 144$–285 keV, with an energy stability of better then 0.1 kV. Figure 1 shows the experimental setup, which was described elsewhere [19,20]. The proton beam (current, about 3–16 μA) passed through two 2 collimators (each 10 mm in diameter) and was focused on the target. The two collimators were located 50 and 100 cm upstream of the target. The proton beam bombarded a 6.3-μg/cm^2-thick natural boron target (80% ^{11}B, 20% ^{10}B), which was made by sputtering natural boron onto a 0.2-mm-thick tantalum backing and was directly water-cooled. An inline Cu shroud cooled to LN_2 temperature (a pipe 4 cm in diameter) extended close to the target for minimizing carbon buildup on the target surface. Together with the target, it constituted the Faraday cup for beam integration. The typical vacuum pressure of the target chamber was about 8×10^{-7} mbar. A negative voltage of 270 V was applied to the pipe to suppress secondary electrons from the target.

A 4×4-fold-segmented, Clover-type, high-purity germanium detector [21,22], which was placed in close geometry at 0°, with its front face at a distance of 29 mm from the target, was utilized for γ-ray detection. The Clover detector has a relative efficiency of about 200% and a typical

*shwxu@impcas.ac.cn

†Present address: Department of Physics, University of Notre Dame, Notre Dame, Indiana 46556, USA.

‡Present address: School of Physics, University of Edinburgh, Mayfield Road, Edinburgh EH9 3JZ, United Kingdom.

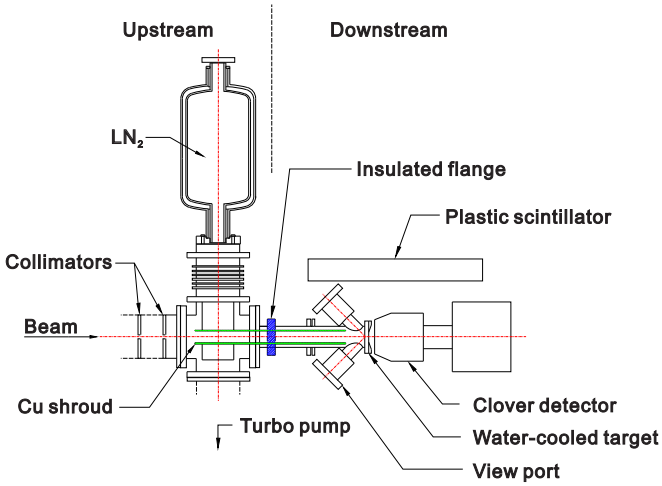

FIG. 1. Schematic of the experimental setup.

resolution of 2.3 keV (at $E_\gamma = 1.3$ MeV). The energy spectra from four germanium crystals were taken simultaneously and then summed up after energy calibration. The performance of this Clover detector was previously studied in both the crystal (singles) and the clover (addback) modes [21,22]. In this work, the crystal mode was chosen to minimize the summing effect of the cascade γ transitions. An EJ-200 plastic scintillator [23] (length, 100 cm; width, 50 cm; thickness, 5 cm) was placed 10 cm above the Clover detector, acting as a veto to suppress the cosmic-ray background. The performance of this veto detector was described elsewhere [20].

The γ-ray efficiency of the Clover detector was carefully calibrated in this work. For low-energy γ rays, the efficiency was calibrated by two standard ^{152}Eu and ^{60}Co sources, with uncertainties of 3.0% and 2.5%, respectively. For high-energy γ rays, the efficiency was determined by use of the well-studied reaction ^{14}N$(p,\gamma)^{15}$O [15]. In this calibration experiment, a 2-mm-thick N_4Si_3 target was bombarded by a 280-keV proton beam. The relative efficiencies of the decay γ rays from ^{15}O at 2373, 5183, 6176, and 6793 keV were normalized to that at 1380 keV, whose absolute efficiency was determined by the standard γ-ray sources mentioned above. Figure 2 shows the absolute efficiencies determined for the Clover detector. The uncertainties ($\sim$5%) of the ^{152}Eu and ^{60}Co data points originate from those of the sources mentioned above, from the systematical ($\sim$4%) and statistical ($\sim$1%) ones. The uncertainties of the ^{14}N$(p,\gamma)^{15}$O data points are of three major origins: (i) uncertainty of the normalized 1380-keV point determined by the sources ($\sim$5%), (ii) statistical uncertainties (2%–10%), and (iii) uncertainties of the γ-ray branching ratios in the compound nucleus ^{15}O (0.7%–3.8% [24]). The simulated efficiencies with the GEANT4 toolkit [25] agree very well with the experimental data for the γ rays beyond 800 keV. The simulated efficiencies are significantly higher than the experimental ones in the low-energy region, probably as a result of the random coincidences with the plastic veto and the relatively low gain in the front-end electronics, and are not shown Fig. 2. Here, we extended the simulation above the maximum experimental data point available at $E_\gamma = 6793$ keV up to 16.5 MeV, which is of interest for the ^{11}B$(p,\gamma)^{12}$C capture reaction.

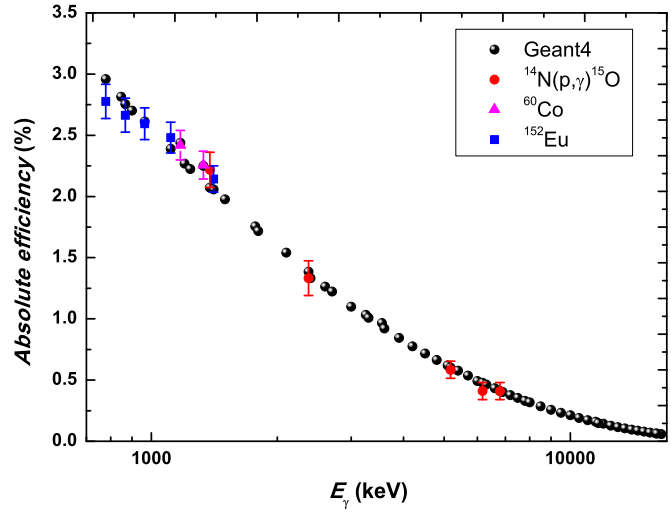

FIG. 2. Absolute efficiencies determined for the Clover detector. Data from the standard sources (^{152}Eu and ^{60}Co) and from the ^{14}N$(p,\gamma)^{15}$O experiment were corrected for the deadtime. The simulated efficiencies with the GEANT4 toolkit are shown for comparison. Note that the (simulated and experimental) efficiencies for ^{60}Co deviate considerably from the general simulation trend, just because the positions of the ^{152}Eu and ^{60}Co sources are a bit different (by 2.5 mm) in the calibration run.

A sample γ-ray spectrum obtained at an energy of $E_p = 171$ keV is shown in Fig. 3. The first-excited-state γ transition (γ_1) and its subsequent decay (γ^*), as well as the ground-state transition (γ_0), were observed clearly in the spectrum. In addition, the location of the 8.69-MeV γ rays, which are emitted in the ^{10}B$(p,\gamma_0)^{11}$C capture reaction, is indicated in the figure. Because of the much smaller cross section of ^{10}B$(p,\gamma_0)^{11}$C [15], no prominent γ peak is observed.

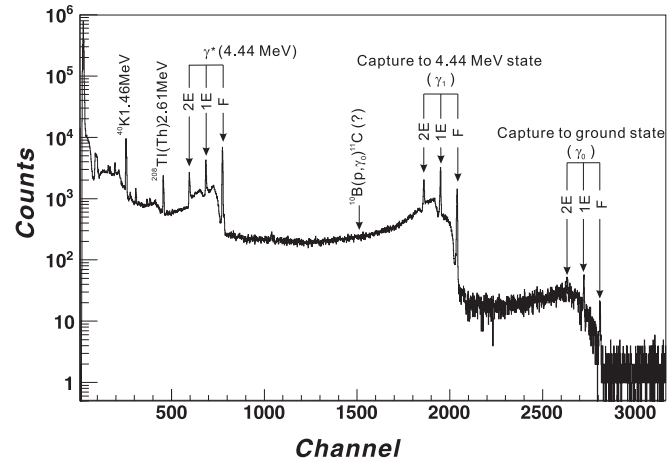

FIG. 3. A sample γ-ray spectrum obtained in the ^{11}B$(p,\gamma)^{12}$C experiment at $E_p = 171$ keV. The capture γ rays populating the ground (γ_0, $\sim$16.1 MeV) and first excited (γ_1, $\sim$11.7 MeV) states of ^{12}C, and those decaying from the first excited state to the ground state (γ^*, 4.439 MeV), are labeled. F, full photo peak; 1E, single-escape peak; 2E, double-escape peak. In addition, the arrow shows where the γ rays emitted from the ^{10}B$(p,\gamma_0)^{11}$C capture reaction ($Q = 8.689$ MeV) should lie.

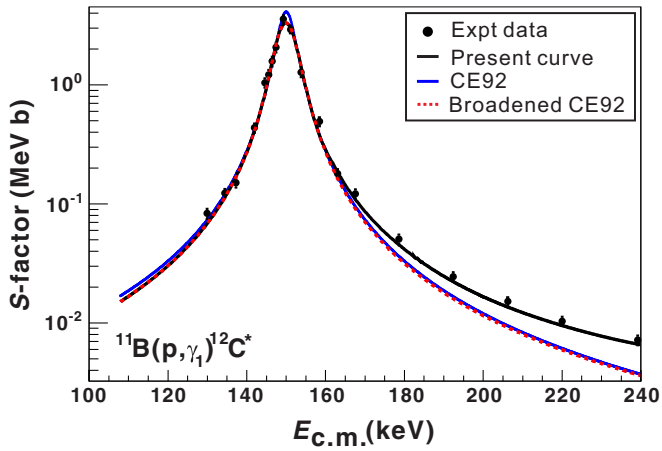

FIG. 4. Astrophysical S factor for the ^{11}B$(p,\ \gamma_1)^{12}$C* reaction channel. The present experimental data have been corrected for the target thickness effect. The result from Cecil *et al.* [12] ("CE92") is represented by the dotted red line. The solid line ("present curve") represents the results calculated by taking the target thickness effect into account. See text for details.

III. RESULTS

The astrophysical S factors of the ^{11}B$(p,\ \gamma_1)^{12}$C* reaction have been determined by measuring the 4.44-MeV γ rays (labeled γ^* in Fig. 3) corresponding to the decay of the first excited state of ^{12}C, as shown in Fig. 4. Here, the angular distribution effect for this γ ray was taken into account based on the previous work [12]. The $E_{\rm c.m.}$ energies were corrected for the target thickness effect as described in Ref. [26]. Here, the major uncertainties originate from those of the statistics (0.5% $\sim$ 4%), beam intensity measured by the Faraday cup ($\sim$5%), efficiency calibration ($\sim$5%), and target thickness ($\sim$10%). Cecil *et al.* [12] derived the simple analytic expression $S = \frac{3\times10^{-5}}{[(E-0.15)^2+7.3\times10^{-6}]}$ (MeV b) (center-of-mass energy E in units of MeV) for the S factor of this capture reaction, which is shown in Fig. 4 as the blue line (labeled "CE92"). In this expression, the true width of the resonance is $\Gamma_{\rm c.m.} = 5.4$ keV, and the peak cross section is $\sigma_1^R = 134 \pm 20\ \mu$b (i.e., an uncertainty of 15%). At the resonance peak, CE92 is higher than the experimental data. In order to compare our experimental data with this analytic expression, an energy broadening [27] of the S factor of Cecil *et al.* with the present target thickness (about 4.3 keV on resonance of 150 keV) was performed, and the result is shown as the dashed red line (labeled "Broadened CE92"). It can be seen that the broadened curve agrees well with the experimental data near the resonance peak. However, this broadening effect becomes small far away from the resonance. As shown in Fig. 4, the present high-energy data deviate from those of CE92, probably because Cecil *et al.* only measured the reaction up to about 165 keV. In order to account for this deviation, an additional polynomial term, $\Delta S = 6.8 - 146.0E + 1255.9E^2 - 5405.3E^3 + 11628.9E^4 + 9998.5E^5$ (MeV b), was added to the above analytic expression. The resulting S-factor expression has been broadened by the target thickness effect, as shown by the solid line (labeled "Present curve"). Thus, for the $(p,\ \gamma_1)$ channel, the S factor (in units of MeV b) derived here can be expressed as $S = \frac{3\times10^{-5}}{[(E-0.15)^2+7.3\times10^{-6}]} + \Delta S$ in the energy region $E = 165$–260 keV, while we adopt the same CE92 S factors in the region below 165 keV.

In addition, a Lorentzian-function fit was done for the experimental data near resonance, which gives a resonance energy (E_R) of 150.0 $\pm$ 0.5 keV and an experimental width of $\Gamma_{\rm exp} = 6.6 \pm 0.5$ keV. Therefore, the true width of the resonance is determined to be 5.0 $\pm$ 0.8 keV by $\Gamma = (\Gamma_{\rm exp}^2 - \Delta E^2)^{1/2}$ [4,5]. Here, ΔE is the proton energy loss [28] in the boron target, about 4.3 $\pm$ 0.4 keV on resonance $E_{\rm c.m.} = 150$ keV. This true width agrees with the value of $\Gamma_{\rm c.m.} = 5.3 \pm 0.2$ keV quoted in the most recent compilation [13]. The resonance properties for the $\sim$150-keV resonance in the ^{11}B $+p$ capture reaction are summarized in Table I.

TABLE I. Resonance properties summarized for the $E_{\rm c.m.} \approx 150$ keV resonance in ^{11}B $+p$ capture.

Ref. No.	E_R (keV)	$\Gamma_{\rm c.m.}$ (keV)	σ_0^R (μb)	σ_1^R (μb)	$\frac{\Gamma_{\gamma_0}}{\Gamma_{\gamma_1}}$ (%)	Target info
[3]	148.5 $\pm$ 1.0	4.9 $\pm$ 1.0				
[4]	149.2 $\pm$ 0.2	4.1 $\pm$ 1.4				Thin & thick
[29]	149.4	4.6	5.5	138		Evaluation
[5]	150.2 $\pm$ 0.3	6.7 $\pm$ 0.5				Thin
[6]	149.4 $\pm$ 0.3	4.6	5.5 $\pm$ 0.8	152 $\pm$ 23		Thick
[7]	149.4				3.3 $\pm$ 1.0	Thick
[8]	149.4	6.7 $\pm$ 0.5 [5]	$\sigma_{(0+1)} = 125 \pm 16$			Thick
		5.0 [6]	$\sigma_{(0+1)} = 167 \pm 22$			Thick
[9]	149.4	6.7 $\pm$ 0.5 [5]			4.6 $\pm$ 0.7	Thick
[10]	149.8 $\pm$ 0.2	5.2 $\pm$ 0.5				Thin
[11]	148.3 $\pm$ 0.1	5.3 $\pm$ 0.2				Thin
[13]	148.6 $\pm$ 0.4	5.3 $\pm$ 0.2	5.5 $\pm$ 0.8	152 $\pm$ 23	4.6 $\pm$ 0.7	Evaluation
[12]	150	5.4	4.5 $\pm$ 0.7	134 $\pm$ 20	3.4	Thick
Present work	150.0 $\pm$ 0.5	5.0 $\pm$ 0.8	6.2 $\pm$ 1.3[b]	134 $\pm$ 20 [12]	4.6 $\pm$ 0.7[a]	Thin

[a]The ratio is adopted from the recent compilation [13]. Here, we obtained a ratio of 4.3% $\pm$ 0.6% measured at $E_{\rm c.m.} \approx 155$ keV, a bit far away from the 150-keV resonance.

[b]Estimated by a compiled branching ratio [13], together with the present σ_1^R value.

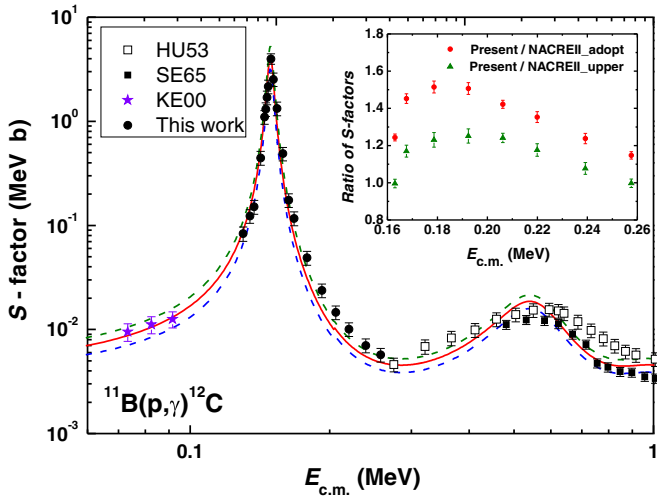

FIG. 5. Astrophysical S factors of $^{11}\mathrm{B}(p,\gamma)^{12}\mathrm{C}$. The previous data, HU53 [6], SE65 [30], and KE00 [14] taken from NACRE II [16], are shown for comparison. Three lines for the potential model (PM) calculations [16] are shown, representing the upper limit, centroid, and lower limit, respectively. Inset: S-factor ratios between this work and NACRE II; filled circles and filled triangles represent the ratios between our data and the values of the adopted (centroid) and upper limits in the compilation, respectively.

The intensity ratio (γ_0/γ_1) between the 16.1-MeV and the 11.7-MeV γ rays is presently determined to be $4.3\% \pm 0.6\%$ at $E_{\mathrm{c.m.}} \approx 155$ keV, which is very much consistent with the most recent evaluation value of $4.6\% \pm 0.7\%$ [13] on the 150-keV resonance. This branching ratio was measured [12] with a thick target to be about $3.7\% \pm 0.5\%$ at 150 keV and $3.5\% \pm 0.5\%$ at 155 keV, respectively, which agree with the present and the evaluation values within the uncertainties. In order to calculate the total cross section (or S factor) of $^{11}\mathrm{B}(p,\gamma_{0+1})^{12}\mathrm{C}$, we have considered the contribution originating from the $^{11}\mathrm{B}(p,\gamma_0)^{12}\mathrm{C}$ channel by adopting the branching ratios of Cecil *et al.*, which were normalized to the compiled value of 4.6% at 150 keV. In fact, this (p,γ_0) channel makes only a very small contribution to the total cross section (or S factor), about 4.3%–9.8% in the energy region of 130–200 keV. The deduced total astrophysical S factors of the $^{11}\mathrm{B}(p,\gamma)^{12}\mathrm{C}$ reaction [(i.e., p,γ_{1+2})] are shown in Fig. 5. Here, additional uncertainties from the (p,γ_0) contribution were added to the data.

Figure 5 shows that our data agree well with those of NACRE II [16] below ~160 keV but deviate considerably from those of NACRE II above this energy. The S-factor ratios between this work and the NACRE II are shown in the inset in Fig. 5, where the filled circles and triangles represent the ratios between our data and the values of the centroid and upper limit adopted in the compilation, respectively. It shows that our data in this energy region are about 15%–50% larger than those centroid values in NACRE II. In addition, our data are also larger than the upper limits of NACRE II in the energy region of 170–240 keV. In terms of the thermonuclear reaction rate of the $^{11}\mathrm{B}(p,\gamma)^{12}\mathrm{C}$ reaction, our new reaction rate is thus enhanced by about 15%–50% compared to the adopted (centroid) rate in NACRE II in the temperature region 0.32–0.62 GK.

IV. CONCLUSION

The absolute cross section of the $^{11}\mathrm{B}(p,\gamma)^{12}\mathrm{C}$ reaction was measured in the energy region $E_{\mathrm{c.m.}} = 130$–257 keV by using a thin target for the first time. The astrophysical S factors of this reaction were determined for capture to the ground (p,γ_0) and first excited (p,γ_1) states of $^{12}\mathrm{C}$. The energy and width derived for the known resonance at ~150 keV agree with the previous results. However, our S factors are about $(15 \sim 50)\%$ larger than the adopted values in NACRE II in the energy region 170–240 keV. According to the present results, this reaction rate is enhanced by about 15%–50% compared to the NACRE II rate in the temperature region 0.32–0.62 GK. This non-negligible correction should be considered in future nucleosynthsis network calculations; it is beyond the scope of this work.

ACKNOWLEDGMENTS

We thank Y. Xu for generously providing the relevant NACRE II data. This work was financially supported by the National Natural Science Foundation of China (Grant Nos. 11490562, 11135005, and 11321064) and the Major State Basic Research Development Program of China (2013CB834406).

[1] D. D. Clayton, *Principles of Stellar Evolution and Nucleosynthesis* (University of Chicago Press, Chicago, 1983).
[2] D. N. Schramm and R. Wagoner, Annu. Rev. Nucl. Sci. **27**, 37 (1977).
[3] R. Tangen, Kgl. Norske. Vid. Sels. Skrifter, NRI (1946).
[4] A. H. Morrish, Phys. Rev. **76**, 1651 (1949).
[5] S. E. Hunt and W. M. Jones, Phys. Rev. **89**, 1283 (1953).
[6] T. Huust and R. B. Day, Phys. Rev. **91**, 599 (1953).
[7] D. S. Craig, W. G. Cross, and R. G. Jarvis, Phys. Rev. **103**, 1414 (1956).
[8] B. D. Anderson *et al.*, Nucl. Phys. A **233**, 286 (1974).
[9] E. G. Adelberge *et al.*, Phys. Rev. C **15**, 484 (1977).
[10] J. M. Davidson *et al.*, Nucl. Phys. A **315**, 253 (1979).
[11] H. W. Becker, C. Rolfs, and H. P. Trautvetter, Z. Phys. A **327**, 341 (1987).
[12] F. E. Cecil *et al.*, Nucl. Phys. A **539**, 75 (1992).
[13] F. Ajzenberg-Selove, Nucl. Phys. A **506**, 1 (1990).
[14] J. H. Kelley, R. S. Canon, S. J. Gaff, R. M. Prior, B. J. Rice, E. C. Schreiber, M. Spraker, D. R. Tilley, E. A. Wulf, and H. R. Weller, Phys. Rev. C **62**, 025803 (2000).
[15] C. Angulo *et al.*, Nucl. Phys. A **656**, 3 (1999).
[16] Y. Xu *et al.*, Nucl. Phys. A **918**, 61 (2013).
[17] L. T. Sun *et al.*, Nucl. Instrum. Methods Phys. Res., Sec. B **263**, 503 (2007).
[18] X. Ma *et al.*, J. Phys.: Conf. Ser. **163**, 012104 (2009).
[19] J. J. He *et al.*, Phys. Lett. B **725**, 287 (2013).

[20] S. Z. Chen *et al.*, Nucl. Instrum. Methods Phys. Res., Sec. A **735**, 466 (2014).
[21] N. T. Zhang *et al.*, Chin. Phys. Lett. **29**, 042901 (2012).
[22] N. T. Zhang *et al.*, J. Phys. G: Nucl. Part. Phys. **40**, 035101 (2013).
[23] ELJEN Technology, http://www.eljentechnology.com/.
[24] F. Ajzenberg-selove, Nucl. Phys. A **523**, 1 (1991).
[25] GEANT4, *a Toolkit for the Simulation of the Passage of Particles through Matter Developed at CERN*; http://geant4.cern.ch/.
[26] C. E. Rolfs and W. S. Rodney, *Cauldrons in the Cosmos* (University of Chicago Press, Chicago, 1988).
[27] K. Spyrou *et al.*, Eur. Phys. J. A **7**, 79 (2000).
[28] O. B. Tarasovab and D. Bazin, Nucl. Phys. A **746**, 411c (2004); http://lise.nscl.msu.edu.
[29] F. Ajzenberg-Selove and T. Lauristen, Rev. Mod. Phys. **24**, 321 (1952).
[30] R. E. Segel, S. S. Hanna, and R. G. Allas, Phys. Rev. **139**, B818 (1965).